COORDINATED GENERATION SCHEDULING OF MICROGRID WITH SMART THERMAL STORAGE USING FUZZY STALKING BASED WOLF ALGORITHM

A.KARTHIKEYAN
Research Scholar
Dept. of Electrical and Electronics Engineering,
College of Engineering Guindy, Anna University,
Chennai, Tamilnadu, India.
akarthikeyan.legs@gmail.com

K.MANIKANDAN
Assistant Professor,
Dept. of Electrical and Electronics Engineering,
Government College of Engineering, Srirangam
Trichy, Tamilnadu, India.
mrmanikandaneee@gmail.com

M.DEVESH RAJ
Associate Professor,
Dept. of Electrical and Electronics Engineering,
SSN college of engineering,
Chennai, Tamilnadu, India.
deveshraj.m@gmail.com

P.SOMASUNDARAM
Associate Professor,
Dept. of Electrical and Electronics Engineering,
College of Engineering Guindy, Anna University,
Chennai, Tamilnadu, India.
somuau77@gmail.com

Abstract: *The energy management system encounters additional challenges while scheduling MicroGrid (MG) with renewable energy sources. Solar and wind generation impose uncertainties due to its sporadic availability. In addition, MG integrated with Smart Thermal Storage (STS) mechanisms like Thermochemical Heat Storage (TCHS) and Ice-Storage Air Conditioner (ISAC) introduces inevitable constraints to the Generation Scheduling (GS) problem. Thereby the GS of STS integrated MG is transformed into Coordinated Generation Scheduling (CGS) by satisfying the electrical, thermal and cooling demand. In this paper, the CGS problem for MG with STS is formulated and solved using the proposed Fuzzy Stalking based Wolf (FSW) algorithm. The proposed FSW algorithm is an improvised Grey Wolf (GW) algorithm based on the incorporation of fuzzy logic in the prey tracking strategy. For an adopted MG with STS, the CGS problem is solved using the proposed FSW algorithms. The simulation results enforce the superiority of the proposed FSW algorithm.*

Key words: *Grey Wolf algorithm, coordinated generation scheduling, fuzzy logic, microgrid, thermal storage.*

1. Introduction

Worldwide policies on economic and environmental electric power production and utilization emphasises on the integration of renewable energy resources into MicroGrid (MG) operation. Among a varied cluster of renewable energy sources, in the state-of-art wind turbines, PV panels and fuel cells have gained significant importance due to their ready availability. Henceforth, integration of wind turbines, PV panels and fuel cells into MG is inevitable. Thereby, optimal MG operation includes several uncertainties and constraints like erratic wind velocity, intermittent irradiation and partial shading due to cloud cover [1]. The implication of effective energy storage mechanism can thwart these uncertainties. In the recent literature [2-6], several Smart Thermal Storage (STS) techniques have evolved for renewable energy integrated MG. Among such STS techniques, latent heat storage [2], Thermochemical Heat Storage (TCHS) [4-6] and Ice-Storage Air Conditioner (ISAC) [7-8] have gained significant importance. The latent heat storage system utilizes the energy exchange caused by the isothermal phase change of certain suitable materials. The chemical storage system employs reversible exothermic synthesis reaction, resulting in exhaustive heat energy production. In contrast absorption based storage system yields relatively less heat energy production but the activation energy requirement for instigating the reaction is comparatively lesser than chemical storage system. The TCHS system utilizes the combined application of absorption phenomenon and reversible chemical reactions for efficient heat production and storage. Thereby, TCHS system requires lesser activation energy and produces high heat energy. The avid benefits of TCHS system are its ability to store relatively high heat energy for a long duration and minimum heat loss. The comparative analysis [3] reports that the heat storage per unit volume capacity of TCHS system is twice that of latent heat storage. Hence in this paper, TCHS is incorporated into the renewable energy integrated MG operation. If the heat energy obtained from the solar collectors is higher than the

corresponding thermal demand then the excess heat energy (after satisfying the thermal demand) is stockpiled in TCHS as available thermal storage (up to its full capacity). Similarly if the purchase cost of grid power is economical and if the available thermal storage is less than its full capacity then the power from the central grid is utilized to stockpile the thermal energy in TCHS. This operating condition of TCHS is termed as mode 1. On the other hand when there is no available thermal storage then the thermal demand is met by either consuming electrical power from the MG (depending upon the energy availability) or consuming electrical power from the central power grid. This condition of TCHS is denoted as mode 2. In contrary if the available thermal storage is higher than the corresponding thermal demand then the entire thermal demand is satisfied by the stored thermal energy in TCHS. This mode of operation is termed as mode 3. Under this circumstance where the entire thermal demand is satisfied by the available thermal storage, neither the MG nor the central power grid supplies electrical power, thereby the stressed operation of MG is subsidised. When the available thermal storage is lesser than the thermal demand, then a portion of thermal demand is met by TCHS from the available thermal storage and the remaining portion of the thermal demand is fulfilled by consuming the electrical power from the MG (depending on the energy availability) or the central power grid. This last mode of operation is named as mode 4. Moreover, in this paper the TCHS system present in the MG utilizes the heat from the solar collectors along with the heat discharged from the high temperature output SOFC fuel cell [9-10].

In recent years the electric power requirement of air conditioning systems imposes a drastic escalation in peak load demand. Eventually under such conditions ISAC is an effective and economic option to temperate the stressful operation of MG. ISAC is an emerging effective cooling storage and supply technology comprising of the following major components: ice-chiller unit for the production of cold air using electric power, ice storage tank for storing the cold air produced by the ice-chiller using anhydrous ammonia, pump and other auxiliary devices. With an intention to simultaneously satisfy the cooling demand along with the transferal of additional power demand (during peak load operation), in this paper ISAC is incorporated into renewable energy integrated MG. Depending on the stress in the MG ISAC promptly operates in any one of the four operating modes namely, air-conditioning mode, ice making mode, ice melting mode and combined mode. ISAC is operated in the air-conditioning mode only when there is no available cold storage. Under this mode the electrical power is drawn either from the MG (depending on the energy availability) or from the central power grid to satisfy the cooling demand. Ice making mode of ISAC is operated only when the available cold storage is less than its full capacity. In this mode the electrical power is drawn either from the MG (depending on the energy availability) or the central power grid (depending on the purchase cost) and it is stored for later use. ISAC functions in the ice melting mode only when the available cold storage is higher than the cooling demand. Under this mode of operation ISAC supplies the entire cooling demand from the available cold storage thereby; neither the MG nor the central power grid supplies electrical power, thereby if this condition persists during the stressed operation of MG the increase in peak electrical demand of MG is relatively relieved. When the available cold storage is lesser than the cooling demand then ISAC merges both air-conditioning mode and ice melting termed as combined mode. In the combined mode of operation a part of cooling demand is supplied by the available cold storage and the remaining portion of the cooling demand is satisfied by drawing the electrical power from the MG (depending on the energy availability) or the central power grid.

For the renewable energy and STS integrated MG, Generation Scheduling (GS) problem encompasses: (i) multiple objective functions like minimization of operating cost in diesel generators, fuel cell and gas turbine; minimization of pollutant emission, along with minimization of purchase cost (from the central power grid) and maximization of revenue in selling power to the central power grid, (ii) multiple demands like electrical, thermal and cooling and (iii) multiple constraints like minimum and maximum generating limits, battery storage limit and its State of Charge (SOC), capacity limits of TCHS and ISAC, electrical power balance (inclusive of thermal and cooling demand satisfaction). Thereby the GS problem is transformed into Coordinated Generation Scheduling (CGS) problem as described in section 2.

Several stochastic optimization techniques [11-16] have been proposed for solving complex power system GS problems. In recent years, swarm based (collective search) optimization techniques (PSO, GW) have gained popularity. Grey Wolf algorithm (GW) is one such collective social behaviour based optimization technique [14-16] which can be effectively employed for solving the proposed CGS problem. The GW

algorithm employs diversification (explorative) and intensification (exploitation) based search procedures to obtain the optimum. However the search methodology of GW algorithm is quite sluggish in approaching the optimal value. Therefore with an intention to enhance the search ability of GW algorithm fuzzy logic approach is appropriately infused into the search procedures thereby the GW algorithm is termed as Fuzzy Stalking based Wolf (FSW) algorithm. The formulation and detailed solution methodology of FSW algorithm is described in section 3. The proposed FSW algorithm is applied to an adopted MG and the optimal solution with discussions are described in section 4. The conclusions drawn from the analysis are listed in section 5.

2. Coordinated Generation Scheduling Problem

The modelling of renewable energy resources, STS and CGS problem formulation is as follows:

2.1 Modelling of renewable energy sources

2.1.1 Wind generation model

Due to sporadic availability of wind, the generation from wind turbine varies as shown in Figure 1. From Figure 1, the power generated from wind turbine P_{wind} is given by,

$$P_{wind}(v)=\begin{cases} P_r\dfrac{v^k-v_c^k}{v_r^k-v_c^k} & (v_c\le v\le v_r)\\ P_r & (v_r\le v\le v_f)\\ 0 & (v<v_c \text{ or } v>v_f)\end{cases} \quad (1)$$

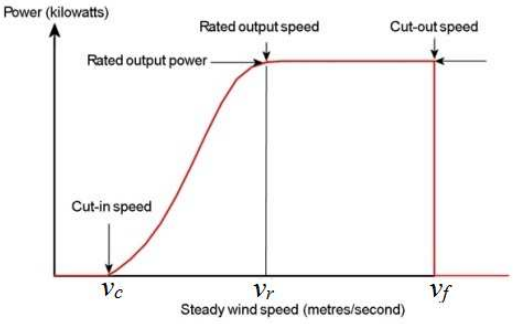

Fig. 1.Wind speed vs Power output

For a time period the wind velocity is predetermined using Weibull distribution [1] and its probability density function $f(v)$ is as follows,

$$f(v)=\frac{k}{c}\left(\frac{v}{c}\right)^{k-1}e^{-\left(\frac{v}{c}\right)} \quad (2)$$

Where,

$$k=\left(\frac{\sigma}{\bar{v}}\right)^{-1.086} \quad (3)$$

$$c=\frac{\bar{v}}{\Gamma\left(1+\frac{1}{k}\right)} \quad (4)$$

2.1.2 PV generation model

The generation from the PV array P_{pv} is modelled as

$$P_{PV}(S)=\eta.I_{real}.V(S,T).N_P.N_S.t_p \quad (5)$$

Where,

$$I_{real}=I(S,T)\times(1-T_C) \quad (6)$$

$$T_C=a.N^2-b.N+c \quad (7)$$

$$I(S,T)=I+\Delta I(S,T) \quad (8)$$

$$\Delta I(S,T)=\alpha_{PV}\left(T+\frac{S}{S_{STC}}(T_{NOR}-T_{STC})-T_{STC}\right)+I\left(\frac{S}{1000}-1\right) \quad (9)$$

$$\Delta V(S,T)=-\beta_{PV}*\left(T+\frac{S}{S_{STC}}(T_{NOR}-T_{STC})-T_{STC}\right)-R_S*\Delta I(S,T) \quad (10)$$

$$V(S,T)=V+\Delta V(S,T) \quad (11)$$

$$I=I_{SC}\left[1-C_1\left(e^{\frac{V}{C_2V_{OC}}}-1\right)\right] \quad (12)$$

$$C_1=\left(1-\frac{I_m}{I_{SC}}\right)e^{-\frac{V_m}{C_2V_{OC}}} \quad (13)$$

$$C_2=\left(\frac{V_m}{V_{OC}}-1\right)\Big/\ln\left(1-\frac{I_m}{I_{SC}}\right) \quad (14)$$

The PV array model [1] includes the effect of uncertainties like partial shading, cloud cover etc.

2.2 Modelling of STS system

2.2.1 Modelling of TCHS

In TCHS there are four modes of operation. The corresponding available thermal storage of TCHS under the various modes is as follows

2.2.1.1 Mode 1 (thermal storage)

$$P(t)_{TCHS}=\begin{cases}P(t-1)_{TCHS}+\{c_p\rho Av^c(T_L-T_0)\} & \text{if } P(t-1)_{TCHS}<P_{TCHS}^{\max}\\ P_{TCHS}^{\max} & otherwise\end{cases} \quad (15)$$

2.2.1.2 Mode 2 (neither thermal storage nor supply)

$$P(t)_{TCHS}=0 \quad (16)$$

2.2.1.3 Mode 3 (complete supply of thermal demand)

$$P(t)_{TCHS}=P(t-1)_{TCHS}-P(t)_{D,ther} \quad (17)$$

2.2.1.4 Mode 4 (partial supply of thermal demand)

$$P(t)_{TCHS}=0 \ \ when \ \ P(t)_{D,ther}-P(t-1)_{TCHS}>0 \quad (18)$$

2.2.2 Modelling of ISAC

In ISAC there are four modes of operation. The corresponding available cooling storage of ISAC under the various modes is as follows

2.2.2.1 Air-conditioning mode (neither cold storage nor supply)

$$P(t)_{ISAC} = 0 \tag{19}$$

2.2.2.2 Ice making mode (cold storage)

$$P(t)_{ISAC} = \begin{cases} P(t-1)_{ISAC} + P^{\max}_{ice-chiller} & if\ P(t-1)_{ISAC} < P^{\max}_{ISAC} \\ P^{\max}_{ISAC} & otherwise \end{cases} \tag{20}$$

2.2.2.3 Ice melting mode (complete supply of cooling demand)

$$P(t)_{ISAC} = P(t-1)_{ISAC} - P(t)_{D,\text{cool}} \tag{21}$$

2.2.2.4 Combined mode (partial supply of cooling demand)

$$P(t)_{ISAC,\text{cm}} = 0 \ \ when\ P(t)_{D,\text{cool}} - P(t-1)_{ISAC} > 0 \tag{22}$$

2.3 Objective function

The mathematical formulation of CGS problem with multiple objectives and constraints are as follows,

2.3.1 Minimization of total operating cost (TC)

$$TC = \sum_{t=1}^{24} OC^t_x + CPE^t - ISE^t \tag{23}$$

Where,

$$x \in \{dg,\ fc, gt, wt,\ pv, TCHS, ISAC\} \tag{24}$$

$$OC^t_{dg,i} = \sum_{i=1}^{ndg} \left(CF_{dg,i} \times P^t_{dg,i} \right) + \left(CM_{dg,i} \times P^t_{dg,i} \right) \tag{25}$$

$$OC^t_{\text{fc},i} = \sum_{i=1}^{nfc} \left(CF_{\text{fc},i} \times P^t_{\text{fc},i} \right) + \left(CM_{\text{fc},i} \times P^t_{\text{fc},i} \right) \tag{26}$$

$$OC^t_{gt,i} = \sum_{i=1}^{ngt} \left(CF_{gt,i} \times P^t_{gt,i} \right) + \left(CM_{gt,i} \times P^t_{gt,i} \right) \tag{27}$$

$$OC^t_{\text{wt},i} = \sum_{i=1}^{nwt} \left(CM_{\text{wt},i} \times P^t_{\text{wt},i} \right) \tag{28}$$

$$OC^t_{\text{pv},i} = \sum_{i=1}^{npv} \left(CF_{\text{pv},i} \times P^t_{\text{pv},i} \right) + \left(CM_{\text{pv},i} \times P^t_{\text{pv},i} \right) \tag{29}$$

$$OC^t_{\text{ISAC}} = \left(CM_{\text{ISAC}} \times P^t_{\text{ISAC}} \right) \tag{30}$$

$$OC^t_{TCHS} = \left(CM_{TCHS} \times P^t_{TCHS} \right) \tag{31}$$

$$CPE^t = C^t_p \times \left(P^t_{CG/MG,ther} + P^t_{CG/MG,cool} + U_{elec} \times P^t_{CG,elec} \right) \tag{32}$$

Where,

$$U_{elec} = \begin{cases} 1\ if\ P^t_{CG,elec} > 0 \\ 0\ otherwise \end{cases} \tag{33}$$

$$ISE^t = C^t_s \times \left(U_{elec} \times P^t_{CG,elec} \right) \tag{34}$$

Where,

$$U_{elec} = \begin{cases} 1\ if\ P^t_{CG,elec} < 0 \\ 0\ otherwise \end{cases} \tag{35}$$

2.3.2 Minimization of toxic emissions (TE)

$$TE = \sum_{i=1}^{N} E^t_y \tag{36}$$

$$y \in \{dg,\ fc, gt\} \tag{37}$$

$$E^t_y = \sum_{i=1}^{ny} \alpha_{y,i} + \beta_{y,i} P^t_{y,i} + \gamma_{y,i} (P^t_{y,i})^2 \tag{38}$$

2.4 Constraints

2.4.1 Power Balance Constraint

$$P(t)_{D,ther} = \begin{cases} -P(t)_{TCHS} + P^t_{CG/MG,ther} & under\ Mode 1 of\ TCHS \\ P(t)_{TCHS} + P^t_{CG/MG,ther} & otherwise \end{cases} \tag{39}$$

$$P(t)_{D,\text{cool}} = \begin{cases} -P(t)_{ISAC} + P^t_{CG/MG,\text{cool}} & under\ ice\ making\ mode\ of\ ISAC \\ P(t)_{ISAC} + P^t_{CG/MG,\text{cool}} & otherwise \end{cases} \tag{40}$$

$$P(t)_{D,\text{elec}} = \sum_{i=1}^{npv} P^t_{pv,i} + \sum_{i=1}^{nwt} P^t_{wt,i} + \sum_{i=1}^{ngt} P^t_{gt,i} + \sum_{i=1}^{nfc} P^t_{fc,i} + \sum_{i=1}^{ndg} P^t_{dg,i} + (\text{c}(t) \times P^t_{batt}) + P^t_{CG,elec} \tag{41}$$

where,

$$c(\text{t}) = \begin{cases} 1 & \text{if battery discharges} \\ -1 & \text{if battery charges} \end{cases} \tag{42}$$

2.4.1.1 Capacity limits

$$0 \le P^t_{pv,i} \le P^{\max}_{pv,i} \tag{43}$$

$$0 \le P^t_{\text{wt},i} \le P^{\max}_{\text{wt},i} \tag{44}$$

$$P^{\min}_{\text{gt},i} \le P^t_{\text{gt},i} \le P^{\max}_{\text{gt},i} \tag{45}$$

$$P^{\min}_{\text{fc},i} \le P^t_{\text{fc},i} \le P^{\max}_{\text{fc},i} \tag{46}$$

$$P^{\min}_{\text{dg},i} \le P^t_{\text{dg},i} \le P^{\max}_{\text{dg},i} \tag{47}$$

$$0 \le P(t)_{TCHS} \le P^{\max}_{TCHS} \tag{48}$$

$$0 \le P(t)_{ISAC} \le P^{\max}_{ISAC} \tag{49}$$

2.4.1.2 SOC limits of battery[1]

$$SOC(\text{t}) = \text{SOC}(\text{t}-1) - \left(\eta_{bc} I_{bc} + \frac{1}{\eta_{bd}} I_{bd} \right) P_{batt}(\text{t}-1) \Delta t / C_b \tag{50}$$

Where,

$$I_{bc} + I_{bd} \in (0,1) \tag{51}$$

$$SOC_{\min} \le SOC(\text{t}) \le SOC_{\max} \tag{52}$$

$$P_{batt}(t) = \begin{cases} SOC(t) \times C_b & if\ SOC_{\min} < SOC(\text{t}) < SOC_{\max} \\ 0 & otherwise \end{cases} \tag{53}$$

3. Solution methodology

3.1 Grey wolf (GW) algorithm for CGS problem

Grey wolf (GW) algorithm attains an optimal solution by modifying a set of initial feasible solution (pack of wolves) over several iterations. Each initial grey wolf among N_{GW} searches for the optimum through tracking, stalking and competitive hierarchy mechanism based hunting.

The various sequential steps for solving the CGS problem using GW algorithm are as follows:

3.1.1 Initialization of grey wolf pack

An initial wolf pack $GW^{j,iter}$ $(j=1,2,....,N_{GW})$ is generated for the first iteration ($iter=0$). The elements of each grey wolf are predetermined wind velocity v, forecasted solar irradiation S, stored thermal energy $(T_L - T_0)$ along with randomly generated (using uniform distribution) power output of ndg diesel generating units, ngt gas turbine units and nfc fuel cells.

$$GW^{j,iter} = [v^t; S^t; (T_L - T_0)^t; P_{dg,1}^{t,j,iter}, P_{dg,2}^{t,j,iter}, ...P_{dg,\text{ndg}}^{t,j,iter}; P_{gt,1}^{t,j,iter}, P_{gt,2}^{t,j,iter}, ...P_{gt,\text{ngt}}^{t,j,iter}; P_{\text{fc},1}^{t,j,iter}, P_{\text{fc},2}^{t,j,iter}, ...P_{\text{fc,nfc}}^{t,j,iter}] \quad (54)$$

For each grey wolf wind power generation (1), solar power generation (5) and stored thermal energy (15-18) are computed.

3.1.2 Evaluation of fitness function value

The fitness function value fit^j for each grey wolf is computed as,

$$fit^{j,iter} = TC^j + k_1 TE^j + k_2 \left| VPB^j \right| \quad (55)$$

Where,

$$VPB^j = \sum_{i=1}^{npv} P_{pv,i}^{t\,j} + \sum_{i=1}^{nwt} P_{wt,i}^{t\,j} + \sum_{i=1}^{ngt} P_{gt,i}^{t\,j} + \sum_{i=1}^{nfc} P_{fc,i}^{t\,j} + \sum_{i=1}^{ndg} P_{dg,i}^{t\,j} + (c(t) \times P_{batt}^{t\,j}) + P_{CG,elec}^{t\,j} - P(t)_{D,\text{elec}} \quad (56)$$

k_1 and k_2 are emission coefficient factor and penalty factor for power balance constraint violation (41). The value of emission coefficient factor is chosen to highlight the effectiveness of pollutant emission. The penalty factor is chosen such that if there is any power balance constraint violation then the fitness value corresponding to that grey wolf is made ineffective.

3.1.3 Tracking

For the next iteration $(iter+1)$ each grey wolf searches for a prey (feasible solution) within its range by exploration mechanism as follows,

$$GW^{j,iter+1} = [v^t; S^t; (T_L - T_0)^t; P_{dg,1}^{t,j,iter+1}, P_{dg,2}^{t,j,iter+1}, .. P_{dg,\text{ndg}}^{t,j,iter+1}; P_{gt,1}^{t,j,iter+1}, P_{gt,2}^{t,j,iter+1}, ..P_{gt,\text{ngt}}^{t,j,iter+1}; P_{\text{fc},1}^{t,j,iter+1}, P_{\text{fc},2}^{t,j,iter+1}, ..P_{\text{fc,nfc}}^{t,j,iter+1}] \quad (57)$$

The elements $X^{j,iter+1} \in \{P_{dg,i}^{t,j,iter+1}; P_{gt,i}^{t,j,iter+1}; P_{\text{fc,i}}^{t,j,iter+1}\}$ pertaining to each set of control variables are computed as,

$$X^{j,iter+1} = X^{j,iter} + \{rand(0,1) \times (X_i^{\max} - X_i^{\min})\} \quad (58)$$

If any of the randomly generated elements at $iter+1$ violates its limit then the value of the violating limit is assigned to the corresponding element. The fitness function value $fit^{j,iter+1}$ of each tracker grey wolf is computed using equation (55). The fitness function value at the present iteration $(iter+1)$ and its previous value $(iter)$ are compared and the best solution is retained (minimum fitness value).

3.1.4 Competitive hierarchy mechanism based hunting

The social hierarchy of the grey wolf pack is established by selecting the alpha (α), beta (β), delta (δ), and other omega (ω) wolves based on the fitness function values. The N_{GW} wolves are arranged in ascending order of their respective fitness value and the first, second and third best solutions are regarded as alpha, beta and delta wolves, while the rest are considered as omega wolves. The hunt (exploitation mechanism) is guided by the alpha wolf and occasionally supported by beta and delta wolves. This search procedure is expressed mathematically as follows,

$$X^{j,iter+1} = X^{\alpha,iter} + \{rand(0,1) \times (X_i^{\max} - X_i^{\min})\} \;;\; j \neq \alpha \quad (59)$$

Where, $X^{\alpha,iter+1} \in \{P_{dg,\text{i}}^{t,\alpha,iter+1}; P_{gt,\text{i}}^{t,\alpha,iter+1}; P_{\text{fc,i}}^{t,\alpha,iter+1}\}$ are the elements pertaining to the alpha wolf.

The evaluation of fitness, tracking and hunting process are repeated until a specified count (maximum iteration). At the end of the maximum iteration, the final solution pertains to the prey located by the alpha wolf.

3.2 Fuzzy Stalking based Wolf (FSW) algorithm for CGS problem

The major drawback of GW algorithm is a very large computation time due to the large number of iterations required to obtain a global optimum. Hence there is a need to accelerate the convergence of the search techniques in GW algorithm. The two primitive search processes namely tracking (exploration) and hunting (exploitation) in GW algorithm are inadequate, hence with a view to obtain faster convergence certain modifications are incorporated in equation (58) by the application of fuzzy based Gaussian distribution. This modified GW algorithm is termed as Fuzzy Stalking based Wolf (FSW) algorithm. In addition the concept of balance between the intensification and diversification search strategies is incorporated in the competitive hierarchy mechanism.

4. Results and discussions

The proposed FSW and GW algorithms are tested on an adapted MG comprising of 8 generating units integrated with 3 storage units. The generating units include PV, wind turbine, gas turbine, fuel cell, diesel generator and the storage units are battery, ISAC, TCHS. The architecture of the MG is shown in Figure 3. The various MG sources and its rating considered for the MG shown in Figure 2 are two PV system with

each rated at 15 kW, one wind turbine rated at 30 kW,

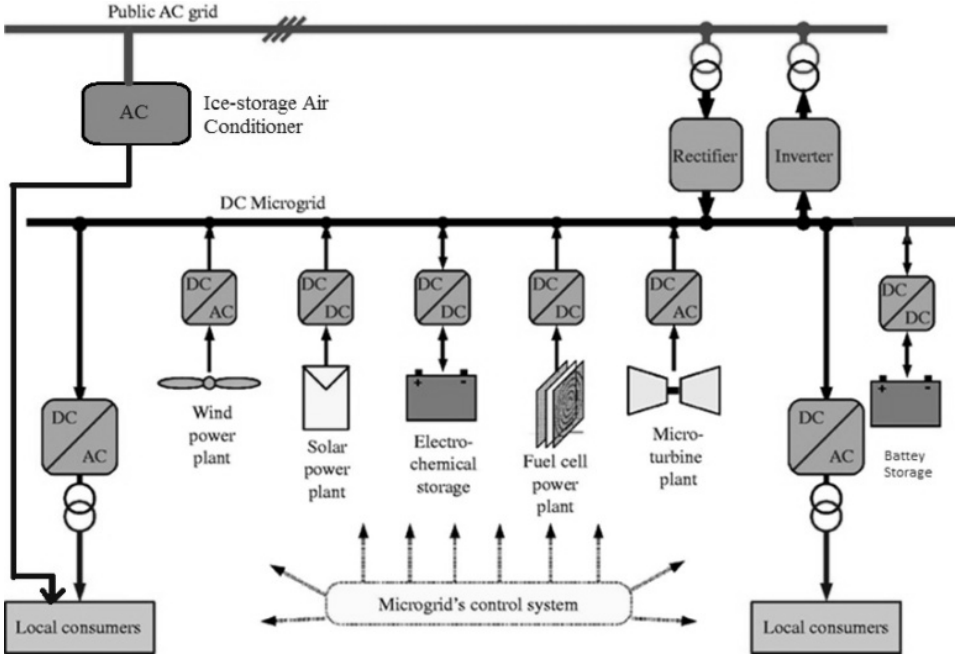

Fig. 2 Architecture of the adapted microgrid

Table 1 Microgrid fuel and maintenance cost data

Cost ($/kw)	PV	WT	GT	FC	DG1	DG2	DG3	ISAC	TCHS
CM	0.0096	0.0296	0.0648	0.0293	0.088	0.088	0.09	0.0098	0.0096
CF	0	0	0.695	0.206	0.396	0.396	0.396	0	0

Table 2 Emissions coefficients of microsources

Emission Coefficient	GT	FC	DG1	DG2	DG3
α_i (kg/hr)	152.04	102.69	36.29	36.29	42.8
β_i (kg/hrkw)	0.0534	0.0445	3.057	3.057	4.542
γ_i (kg/hrkw^2)	12.7928	0.6396	632.604	632.604	645.396

one gas turbine rated at 30 kW, one fuel cell rated at 30 kW and three diesel generators with each unit rated at 30kW, 30kW, 60kW. The total system generation capacity is 240 kW.

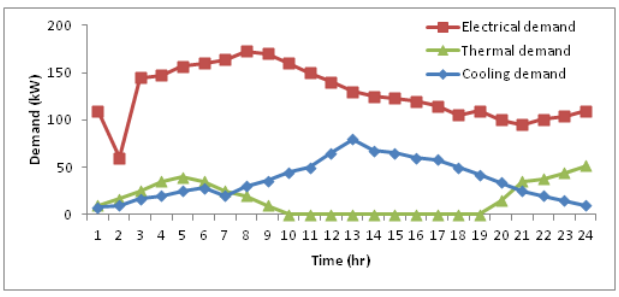

Fig. 3 Various load profile of microgrid

The CM and CF are presented in Table 1 and emission coefficients are presented in Table 2.

The MG comprises of one battery storage with 30 kW capacity. The capacity of the Ice-storage air conditioner is 200 kW. The capacity of the thermo-chemical heat storage is 100 kW. The multiple demands of the MG namely electrical, thermal and cooling are shown in Figure 3.

The purchase and selling cost of central power grid are presented in Table 3.

The irradiation value and the mean air temperature value for solar power generation are pre-specified [17] as shown in Table 4.

Using the pre-specified values as in Table 4, the

solar power is predicted using equations (5-14) and shown in Figure 4. For TCHS the input temperature of the heat exchanger is obtained from Table 4 and the output temperature of the heat exchanger is 30 percentage of its corresponding input temperature.

The wind velocity for the wind turbine is pre-specified as shown in Table 5. The cut in, rated and cut out wind velocities are 2.5, 6.5 and 10 m/s respectively.

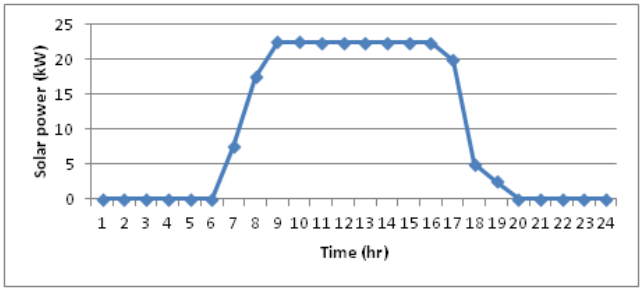

Fig. 4 Solar power generation

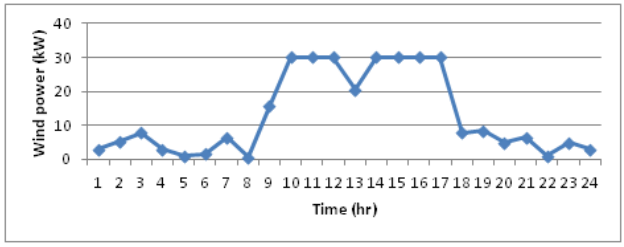

Fig. 5 Wind power generation

Using the pre-specified values as in Table 4, the wind power is predicted using equations (1-2) and shown in Figure 5.

For the consider MG system N_{GW} is chosen as 50. The penalty factors k_1 and k_2 are chosen by trial and error. Initially a small value between 10 and 100 will be chosen. After the investigation if the constraint violated grey wolves have not been effectively eliminated then, the penalty factor values will be increased until a converged solution is reached with no constraint violations. Convergence is tested for 100 trial runs. The fuzzy stalking data are presented in Table 6.

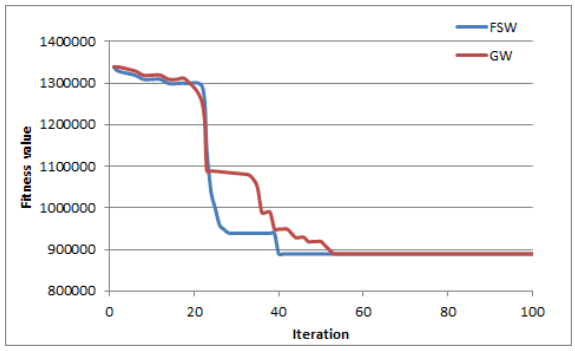

Fig. 6 Convergence characteristic of GW and FSW algorithms for CGS problem

The convergence characteristic of adapted microgrid corresponding to GW and FSW algorithms based CGS problem is shown in Figure 6. The convergence characteristic is drawn by plotting the minimum fitness value across iteration index.

From Figure 6 it is absorbed that the fitness converges smoothly to the optimum value without any hasty oscillations, thus confirming convergence reliability of the proposed algorithm moreover FSW algorithm has much better convergence than GW algorithm.

The optimal solution of adapted microgrid system for CGS problem using the proposed FSW algorithm is compared with GW algorithm and the results for the initial period (t=1) are presented in Table 7. The optimal solution for the entire 24 hour interval is presented in Table 8. From Table 7 it can be inferred that the optimal solution lie within the feasible limits and satisfies the power balance constraints. Thus it can be observed that the proposed algorithm effectively eliminates the inequality limit violations. The SOC of the battery for a 24 hour interval is shown in Figure 7.

Table 3 Grid power exchange cost

Hour	1	2	3	4	5	6	7	8	9	10	11	12
Purchase cost ($/kW)	1.4	1.5	1.7	1.65	1.7	2	2.15	2.35	2.55	2.6	2.7	3
Selling cost ($/kW)	1.2	1.3	1.4	1.5	1.6	1.9	2.1	2.1	2.11	2.3	2.5	2.9
Hour	13	14	15	16	17	18	19	20	21	22	23	24
Purchase cost ($/kW)	3.35	3.05	2.95	2.75	2.55	2.5	2.4	2.3	1.6	1.5	1.45	1.4
Selling cost ($/kW)	3.12	3.01	2.9	2.7	2.4	2	1.85	1.45	1.45	1.4	1.4	1.3

Table 4 Solar irradiation and mean air temperature

Hour	Irradiation (W/m^2)	Mean Air temperature (°C)	Hour	Irradiation (W/m^2)	Mean Air temperature (°C)
1	0	23.7	13	19.5	30.3
2	0	23.4	14	20.9	30.4
3	0	23.1	15	25.8	30.1
4	0	22.9	16	28.4	29.5
5	0	22.7	17	22.5	28.6
6	0	22.6	18	21.8	27.3
7	8.5	22.6	19	15.8	26.4
8	12	23.8	20	0	25.9
9	14	25.9	21	0	25.5
10	14	27.7	22	0	25.1
11	15	29.1	23	0	24.7
12	17.1	29.9	24	0	24.1

Table 5 Wind speed data

Hour	Wind speed(m/s)	Hour	Wind speed(m/s)	Hour	Wind speed(m/s)	Hour	Wind speed(m/s)
1	3.3	7	4	13	5.7	19	4.3
2	3.8	8	2.3	14	8.5	20	3.7
3	4.2	9	5.2	15	8.9	21	4
4	3.3	10	6.7	16	9.3	22	2.4
5	2.4	11	6.8	17	6.5	23	3.7
6	3	12	6.8	18	4.2	24	3.3

Table 6 Data for Fuzzy Stalking

Fuzzy Set	Input1	Input2 for Gas turbine	Input2 for Fuel cell	Input2 for Diesel generators 1&2	Input2 for Diesel generator 3	Output
XSmall	0.00001 to 0.00004	5 to 10	6 to 12	7 to 13	10 to 22	0.001 to 0.005
Small	0.00003 to 0.006	8 to 15	9 to 17	10 to18	20 to 35	0.004 to 0.06
Medium	0.005 to 0.05	12 to 18	14 to 22	15 to 23	33 to 43	0.04 to 0.08
Large	0.03 to 0.5	16 to24	20 to 26	21 to 27	40 to 53	0.075 to 0.09
XLarge	0.4 to 1	22 to 30	24 to 30	25 to 30	50 to 60	0.085 to 0.1

Moreover from table 8 it is inferred that for the same optimum the no of iterations and its corresponding cpu time (computation time) are low for FSW algorithm than GW algorithm. The computation time taken by the proposed FSW algorithm is 85 % of the time taken by GW algorithm. From Figure 3 and Figure 7 it can be inferred that the battery is capable of delivering power during the peak load demand thereby comforting the stress level of the MG.

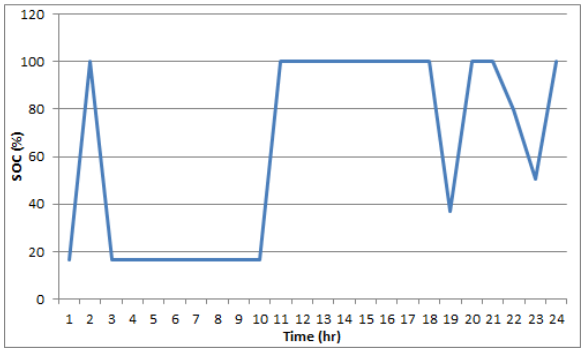

Fig. 7 SOC of the battery during 24 hours interval

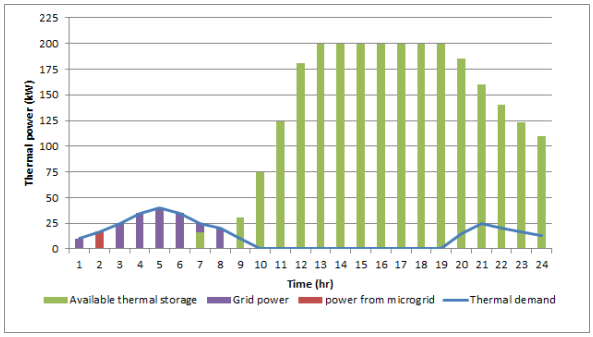

Fig. 8 Thermal load and its generation profile

The combined profile for the thermal demand and its generation is shown in the Figure 8. From figure 8 it can be inferred that during hour 2 the entire thermal demand is sastisfied by drawing power from the microgrid. In contrary during hours 1,3,4,5 and 6 the entire thermal demand is satisfied by drawing power from the central power grid.

In addition as the day proceeds (hours 7) it is observed that TCHS partially satisfies the thermal demand and in the subsequent hours 8,9,20,21,22,23 and 24 TCHS completely satisfies the thermal demand. In hours 10 to 19 (mid-day) there is no thermal demand hence TCHS stores the thermal energy to be utilized at a later duration. During the late evening (hours 20 to 24) as the thermal demand increases, TCHS supplies it from its available stored thermal energy thereby facilitating economic and stress free power system operation.

The combined profile for the cooling demand and its generation is shown in Figure 9. From Figure 9 it can be inferred that during hours 1 to 11 and hours 15 to 24 the entire cold demand is sastisfied by drawing power from the central power grid. From Table 3 and Figure 9 it can be inferred that during hours 1,2,3,21,22 and 23 ISAC draws power from the central power grid for cold storage as the grid power purchase cost is relatively minimal. In addition as the day proceeds (hours 12 and 13) it is observed that ISAC completely satisfies the cooling demand without any aid from the central power grid. In the subsequent hour (hour 14) ISAC partially satisfies the cooling demand, thereby facilitating economic and stress free power systemoperation.

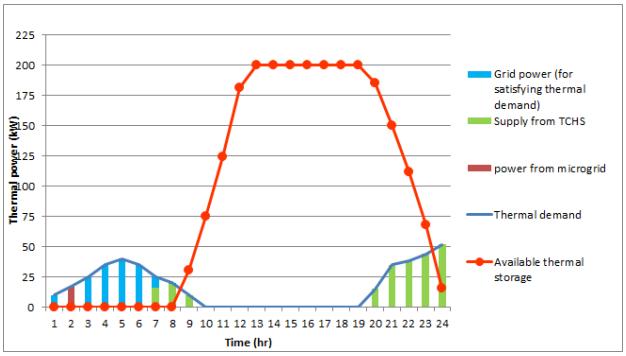

Fig. 9 Cooling demand and its generation profile

The combined profile for the electrical demand and its generation is shown in the Figure 10. From Figure 10 it can be inferred that for the entire duration (hours 1 to 24) the electrical demand corresponding to each hour is satisfied by the combined generation from microsources, battery energy storage system and central power grid.

It can be observed from Figure 10 that during hours 2, 11, 12 to 18, 20, 21 and 24 the entire electrical demand is supplied by the microgrid generation without the aid of the central power grid. Moreover from Figure 10 it is inferred that grid power is negative during hours 2, 12, 13, 14, 15, 16, 17, 18, 20, 21 and 24 denoting that during these hours the excess microgrid generation is sold to the central power grid.

This falicitates economic microgrid operation. By comparing Figure 7 and Figure 10 it can be inferred that during hours 3, 19, 22 and 23 battery discharges to satisfy the electrical demand, thereby reducing the power consumption from the central power grid.

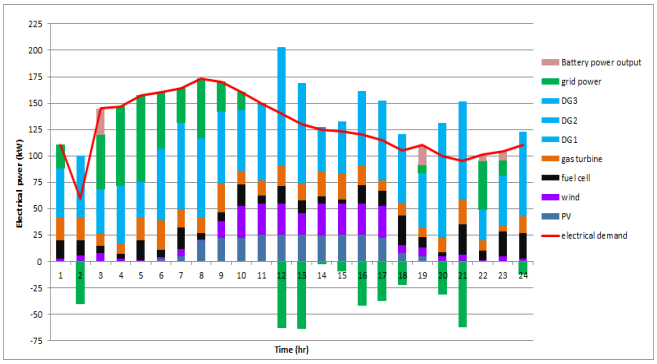

Fig. 10 Electrical Load and Generation Profile

Table 7 Optimal solution of CGS problem for the first hour

Algorithm	FSW	GW
PV generation (kW)	0	0
Wind generation (kW)	2.8703	2.8703
P_{fc} (kW)	17.3779	17.3778
P_{gt} (kW)	21.8414	21.8415
$P_{dg,1}$ (kW)	11.3147	11.3145
$P_{dg,2}$ (kW)	18.4016	18.4017
$P_{dg,3}$ (kW)	16.7375	16.7374
Total P_{dg} (kW)	46.4538	46.4536
Battery power output(kW)	0	0
Total generation from microgrid (kW)	88.5434	88.5432
Grid power for satisfying electrical demand (kW)	21.4566	21.4568
Electrical demand (kW)	110	110
P_{ISAC} (kW)	0	0
Cooling demand (kW)	8	8
P_{TCHS} (kW)	0	8
Thermal demand (kW)	10	10
Total cost ($)	195.6231	195.6234
Total emission (kg/hr)	202.8429	202.8433

Table 8 Optimal generation schedule

Algorithm	Total cost ($)	Total emission (kg/hr)	No. of iterations for convergence	Computation time (ms)
FSW	8004.9830	8812.84	40	10.3
GW	8004.9835	8812.87	60	12.1

5. Conclusion

This paper presents an effective solution methodology for CGS problem of MG integrated with Smart Thermal Storage (STS) mechanisms like TCHS and ISAC. In this paper, the CGS problem for MG with STS is formulated and solved using the proposed Fuzzy Stalking based Wolf (FSW) algorithm by satisfying the electrical, thermal and cooling demand. The proposed FSW algorithm is an improvised Grey Wolf (GW) algorithm based on the incorporation of fuzzy logic in the prey tracking strategy. For an adopted MG with STS, the CGS problem is solved using the proposed FSW algorithms. The simulation results enforce the superiority of the proposed FSW algorithm as it obtains the optimum with reduced computational effort and without any constraints violations.

References

[1] Zhou, T., Sun, W.: *Optimization of Battery–Supercapacitor Hybrid Energy Storage Station in Wind/Solar Generation System*. In: IEEE Transactions on Sustainable Energy, 5 (2014), no.2, Apr 2014, p. 408-415.

[2] Utlu, Z., Aydın, D., Kincay, O.: *Comprehensive thermodynamic analysis of a renewable energy sourced hybrid heating system combined with latent heat storage*. In: Energy Conversion and Management, 84 (2014), Aug 2014, p. 311–325.

[3] Tatsidjodoung, P., Pierres, N., Luo, L.: *A review of potential materials for thermal energy storage in building applications*. In: Renewable and Sustainable Energy Reviews, 18 (2013), Feb 2013, p. 327–349.

[4] Aydin, D., Casey, S.P., Riffat, S.: *The latest advancements on thermochemical heat storage systems*. In: Renewable and Sustainable Energy Reviews, 41 (2015), Jan 2015, p. 356–367.

[5] Jong, A., Trausel, F., Finck, C., Vliet, L., Cuypers, R.: *Thermochemical heat storage system design issues*. In: Science direct, Energy Procedia 48 (2014), p. 309 – 319.

[6] Pardo, P., Deydier, A., Anxionnaz-Minvielle, Z., Rougé, S., Cabassud, M., Cognet, P.: *A review on high temperature thermochemical heat energy storage*. In: Renewable and Sustainable Energy Reviews, 32 (2014), Apr 2014, p. 591–610.

[7] Bao, Z., Zhou, Q., Yang, Z., Yang, Q., Xu, L., Wu, T.: *A Multi Time-Scale and Multi Energy-Type Coordinated Microgrid Scheduling Solution-Part I: Model and Methodology*. In: IEEE Transactions on Power Systems, vol. 30, no. 5, p. 2257-2266, 2015.

[8] Bao, Z., Zhou, Q., Yang, Z., Yang, Q., Xu, L. and Wu, T. *A Multi Time-Scale and Multi Energy-Type Coordinated Microgrid Scheduling Solution-Part II: Optimization Algorithm and Case Studies*. In: IEEE Transactions on Power Systems, 30 (2015), no.5, Sept 2015, p. 2267-2277.

[9] Costamagna, P., Giorgi, A., Magistri, L., Moser, G., Pellaco, L., Trucco, A.: *A Classification Approach for Model-Based Fault Diagnosis in Power Generation Systems Based on Solid Oxide Fuel Cells*. In: IEEE Transactions on Energy Conversion, 31 (2016), no. 2, Jun 2016, p. 676-687.

[10] Akikur, R.K., Saidur, R., Ping, H.W., Ullah, K.R.: *Performance analysis of a co-generation system using solar energy and SOFC technology*. In: Energy Conversion and Management, 79 (2014), Mar 2014, p. 415–430.

[11] Somasundaram, P., Kuppusamy, K.: *Application of Evolutionary programming to security constrained Economic Dispatch*. In: International Journal of Electrical Power and Energy Systems, 27 (2005), no. 5-6, Jun-Jul 2005, p. 343-351.

[12] Pourmousavi, A.S., Nehrir, M.H., Colson, C.M., Wang, C.: *Real-Time Energy Management of a Stand-Alone Hybrid Wind-Microturbine Energy System Using Particle Swarm Optimization*. In: IEEE Transactions on Sustainable Energy, 1 (2010), no. 3, Oct 2010, p. 193-201.

[13] Ramesh, V., Jayabarathi, T., Samarth Asthana., Shantanu Mital, Sampurna Basu.: *Combined Hybrid Differential Particle Swarm Optimization Approach for Economic Dispatch Problems*. In: Taylor and Francis, 38 (2010), no 3, Mar 2010, p. 545-557.

[14] Jayakumar, N., Subramanian, S., Ganesan, S., Elanchezhian, E.B.: *Grey wolf optimization for combined heat and power dispatch with cogeneration systems*. In: International journal of Electrical Power & Energy Systems, 74 (2016), Jan 2016, p. 252–264.

[15] Sharma, S., Bhattacharjee, S., Bhattacharya, A.: *Grey wolf optimization for optimal sizing of battery energy storage device to minimize operation cost of microgrid*. In: IET Generation, Transmission & Distribution, 10 (2016), no. 3, p. 625–637.

[16] Mirjalili, S., Mirjalili, S.M., Lewis, A.: *Grey Wolf Optimizer*. In: Advances in Engineering Software, 69 (2014), Mar 2014, p. 46–61.

[17] *Solar radiation hand book.* Solar energy centre MNRE & Indian metrological department, 2008.

[18] Pavan Kumar, A.V, Alivelu M Parimi: *Digital Simulation of Voltage Regulated Inverter for FLC Controlled Autonomous PV-Wind Hybrid Power System.* In: Journal of Electrical Engineering, 17 (2017), No. 2, p. 323 - 331.

[19] Nouha Nasri, Souhir Tounsi: *Design and optimization of renewable energy structure.* In: Journal of Electrical Engineering, 17 (2017), No. 2, p. 383 - 395.

Appendix A: Nomenclature

P_r	Rated power of the wind turbine
v	Wind speed for a given period
k , c	Scale and shape parameters of weibull distribution
$\Gamma()$	Gamma function
α_{PV}	Short circuit temperature coefficient of PV array
β_{PV}	Open circuit temperature coefficient of PV array
T_c	Weakening coefficient
N_P , N_S	No of PV array in Parallel and series
t_p	Total local peak sunshine hours
a, b	Empirical coefficients
R_s	Series Resistance of PV array
T_{NOR} , T_{STC}	Nominal and Standard working temperature of PV array
S	Solar radiation density (W/m^2)
I_{SC} , V_{OC}	Short circuit current and open circuit voltage of PV array
I_m , V_m	Maximum current and voltage of the

	PV array
P_{TCHS}	kW equivalent of stored thermal energy in TCHS
T_0 , T_L	Output and Input temperature of the heat exchanger
C_P	Specific heat coefficient of heat exchanger coolant
ρ , v^c	Density of heat exchanger coolant and Flow speed (m/s)
A	Cross section of heat exchanger tube
$P_{ISAC,ac}$	Power taken from the central power grid during air conditioning mode
$P_{ISAC,im}$	Power stored in ISAC during ice melting mode
$P_{ic,\max}$	Maximum cooling power generated by ice chiller
OC_x^t	Operating & maintenance cost of xth generating unit at tth hour
CPE^t	Cost of purchase electricity at tth hour
ISE^t	Income of sold electricity at tth hour
CF_i	Cost of fuel of ith generating unit
CM_i	Maintenance cost of ith generating unit
C_p^t , C_s^t	purchase and selling cost at tth hour
E_y^t	Toxic emissions of yth generating unit at tth hour
$\alpha_i, \beta_i, \gamma_i$	Emission coefficients of ith generating unit
$P_{x,i}^t$	Power provided by ith x system $x \in \{dg, fc, gt, wt, pv, TCHS, ISAC\}$ at tth hour
P_{batt}^t	Power provided by battery energy storage system at tth hour
$P_{CG,elec}^t$	Power drawn from central power grid at tth hour for satisfying electrical demand
$P(t)_{D,x}$	$x \in \{ther, cool, elec\}$ thermal, cooling and electrical demand at tth hour
$SOC(t)$, C_b	State of charge of the battery at tth hour and Battery capacity in kWh's
η_{bc}, η_{bd}	Charging & discharging efficiency of the battery
VPB^j	Violation in power balance of jthgrey wolf
$rand(0,1)$	Uniform distribution based random number between the interval 0 to 1
$Nrand(0, \sigma_{X_i}^2)$	Gaussian distribution based random number with zero mean and $\sigma_{X_i}^2$ variance